Chapter 4

Leptonic CP Violation and Mass-Hierarchy in T2K-II, NOνA-II and JUNO

4.1 Introduction

The sensitivity of the A-LBL experiments such as T2K and NOνA to $\delta_{\rm CP}$ and MH can be understood via the following expression of the so-called CP asymmetry [1] presenting a relative difference between $P_{(\nu_\mu \to \nu_e)}$ and $P_{(\bar{\nu}_\mu \to \bar{\nu}_e)}$ near the oscillation maximum, corresponding to $\frac{|\Delta m^2_{31}|L}{4E_\nu} = \pi/2$.

$$\mathrm{A_{CP}}\left(\frac{|\Delta m^2_{31}|L}{4E_\nu} = \pi/2\right) = \frac{P_{(\nu_\mu \to \nu_e)} - P_{(\bar{\nu}_\mu \to \bar{\nu}_e)}}{P_{(\nu_\mu \to \nu_e)} + P_{(\bar{\nu}_\mu \to \bar{\nu}_e)}} \sim -\frac{\pi \sin 2\theta_{12}}{\tan\theta_{23} \sin 2\theta_{13}} \frac{\Delta m^2_{21}}{|\Delta m^2_{31}|} \sin\delta_{\rm CP} \pm \frac{L}{2800km}, \quad (4.1)$$

where $+(-)$ sign is taken for the *normal* (*inverted*) MH respectively. The relation shows that the matter effect due to the baseline (L), in the second term, produces a fake asymmetry along with the intrinsic CP violation asymmetry due to δ_{CP}. With longer baselines the asymmetry due to matter effects dominates over that of δ_{CP}. Figure 4-1 shows the baseline dependence of A_{CP} with matter effect. It is inevitable to remove the effect of the fake asymmetry caused by matter effect unless the baseline is very short. This will be the window to measure $\sin\delta_{CP}$.

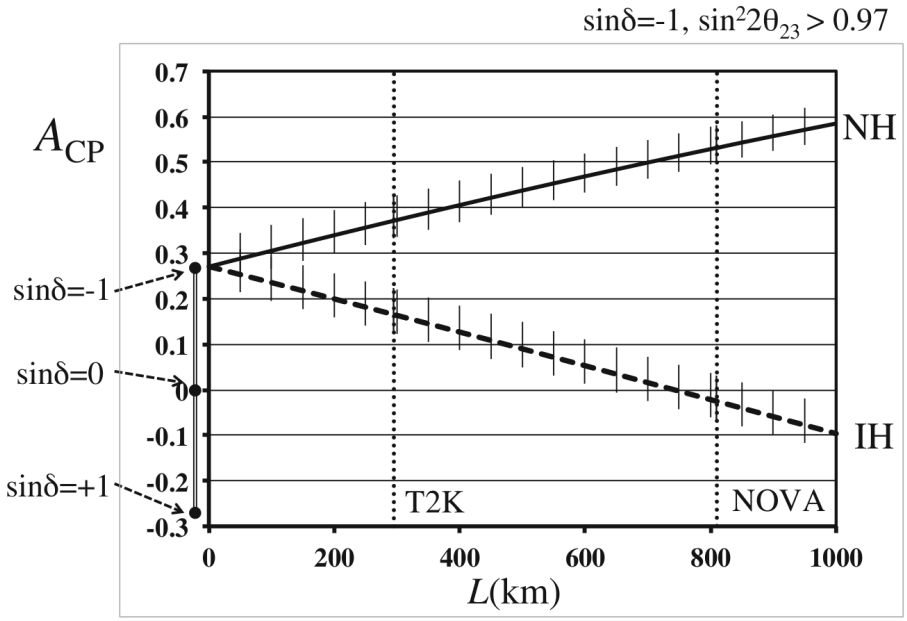

Figure 4-1: Baseline dependence on A_{CP}. The thin vertical lines show the ambiguity from the θ_{23} octant degeneracy. The positions of the intercept at $L = 0$ for $\sin\delta_{CP} = 0, \pm 1$ are shown [1] .

By combining experiments at different baselines, it is possible to know the mass hierarchy and obtain the genuine CP asymmetry. Moreover, the antineutrino-nucleus cross-sections are one-third of the neutrino-nucleus cross-sections, and as such, three times antineutrino flux is necessary to obtain equivalent statistical uncertainties for the ν_e event detection. Therefore, a very high neutrino flux and a large detector mass are necessary to measure the CP violation. Upcoming experiment T2HK is considering the method to emphasize on the problem.

Determining the Δm^2_{31} mass hierarchy is an important next experimental target, not only for the CP asymmetry measurement, but because it is related to the lower limit of the absolute neutrino masses. With values listed in Table 2.1, Equation 4.1 gives $\frac{\pi \sin 2\theta_{12}}{\tan\theta_{23} \sin 2\theta_{13}} \frac{\Delta m^2_{21}}{|\Delta m^2_{31}|} \sim 0.256$, which means the CP violation effect can be observed somewhat between -25.6% and $+25.6\%$. For a 295 km baseline of the T2K experiment, mass hierarchy effect is subdominant with $\sim 10.5\%$. T2K uses a near detector complex, situated 280 m from the production target to constrain the neutrino flux and the neutrino interaction model.

A longer baseline allows NOνA to explore the MH with high sensitivity via the matter effect on the (anti-)neutrino interactions. From Eq. 4.1, it can be estimated that the matter effect in NOνA is $\sim 28.9\%$, which is slightly higher than the CP

violation effect. However, these two effects, along with the ambiguity of the θ_{23} octant, are largely entangled. In other words, NOνA sensitivity on the neutrino MH depends on the value of $\delta_{\rm CP}$. From Figure 2-4, we observe that the separation between NH and IH of NOνA is larger compared to T2K. his is a manifestation of the increased matter effect because of the longer baseline in NOvA.

NOνA's recent data [2] does not provide as much preference to the neutrino mass hierarchy as T2K [3] does since NOνA data shows no indication of the CP violation. As in NuFIT 5.0 data, the best fit in the global analysis remains for the normal mass hierrachy. Without the atmospheric experiment SK, IH rejection is poor with a value of $\Delta\chi^2 = 2.7$ only, which is equivalent to 1.6σ C.L. The result is driven by the updated data from A-LBL T2K and NOνA. However, driven by the better compatibility between the $\Delta m^2_{31(2)}$ determined in ν_μ ($\bar{\nu}_\mu$) disappearance at A-LBL experiments and $\bar{\nu}_e$ disappearance at reactors, the combined global analysis favours NH. If atmospheric data from SK is considered in the global analysis, IH is rejected with a improved sensitivity of $\Delta\chi^2 = 7.3$, which is equivalent to 2.7σ C.L..

The measurement of δ_{CP} mostly comes from the A-LBL experiments. The best fit for the CP violating phase is now favoured at $\delta_{CP} = 195°$. Compared to NuFIT 4.1, the allowed range of δ_{CP} has moved towards CP conserving value. the CP conserving value is now favoured at 0.6σ irrespective of the SK data. If we restrict the mass hierarchy to IO, the best fit of δ_{CP} remains close to $\frac{3\pi}{2}$, CP symmetry being maximally violated. In such case, CP conserving values are rejected at about 3σ.

Unlike the methods exploited by accelerator experiments, a different technique of resolving the MH can give a better resolution to the leptonic CP violation measurement.

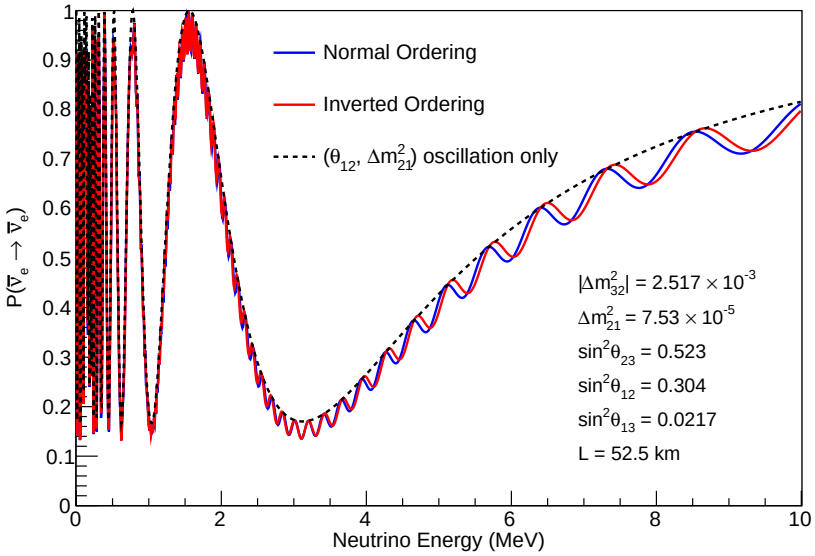

Figure 4-2: Electron antineutrino disappearance probability for JUNO.

4.1.1 Importance of JUNO

There is another method to determine the mass hierarchy by reactor based experiments. The reactor-based medium baseline experiment JUNO primarily aims to determine the MH by measuring the surviving $\overline{\nu}_e$ spectrum, which uniquely displays the oscillation patterns driven by both solar and atmospheric neutrino mass-squared splittings [4]. This feature can be understood via the $\bar{\nu}_e$ disappearance probability in vacuum expressed as follow:

$$P_{(\bar{\nu}_e \to \bar{\nu}_e)} = 1 - \cos^4\theta_{13}\sin^2 2\theta_{12}\sin^2\Phi_{21} - \sin^2 2\theta_{13}\left(\cos^2\theta_{12}\sin^2\Phi_{31} + \sin^2\theta_{12}\sin^2\Phi_{32}\right) \quad (4.2)$$

where $\Phi_{ij} = \frac{\Delta m^2_{ij} L}{4E_\nu}$. An averaged 52.5 km baseline of the JUNO experiment is to obtain the maximum oscillation corresponding to $\Phi_{21} = \pi/2$ around 3 MeV, and relatively enhances the oscillation patterns driven by Φ_{31} and Φ_{32} terms. If the energy spectrum is analyzed the Fourier analysis with a parameter $1/E_\nu$, three peaks at $|\Delta m^2_{21}|$, $|\Delta m^2_{31}|$ and $|\Delta m^2_{32}|$ are observed in the frequency space. The Δm^2_{21} peak locates much lower than the Δm^2_{31} and Δm^2_{32} peaks in the frequency and be distinguished very easily. Since, $\sin^2\theta_{12} \sim 0.3$ and $\sin^2\theta_{12} < \cos^2\theta_{12}$, the amplitude of the terms containing $\sin\Phi_{31}$ is larger than that of $\sin\Phi_{31}$. This means the larger peak corresponds to $|\Delta m^2_{31}|$ and the smaller peak corresponds to $|\Delta m^2_{32}|$.

If the higher frequency peak is larger than that of the lower frequency peak, it means $|\Delta m^2_{31}| > |\Delta m^2_{32}|$, it corresponds to the normal hierachy, and vice versa. To attain it, a very good resolution is still required for the neutrino detector. The oscillation behaviour of JUNO to $\bar{\nu}_e$ disappearance is shown in Figure 4-2.

4.2 Method of χ^2 analysis

We use the following χ^2 function for LBNEs in our analysis.

$$\chi^2 = Min_{\zeta_s,\zeta_b}\Big[2\sum_{i=1}^{n}(N_i^{test} - N_i^{true} - N_i^{true}\ln\frac{N_i^{test}}{N_i^{true}}) + \zeta_s^2 + \zeta_b^2\Big] \tag{4.3}$$

$$N_i^{test}(\zeta_s,\zeta_b) = N_i^{pr}[1+s^s] + N_i^b[1+s^b] \text{ and } N_i^{true} = N_i^{ex} + N_i^b \tag{4.4}$$

where,

- N_i^{pr} is the predicted no. of signal events in the i-th bin for a set of oscillation parameters.
- N_i^b is the no. of charged current backgrounds and NC backgrounds do not depend on the oscillation parameters.
- N_i^{ex} is the no. of observed current signal events in the i-th bin.
- The quantities s^s and s^b are the systematic (normalisation) errors on the signal and background respectively.
- The quantities ζ_s and ζ_b are the "pulls" due to systematic error on signal and background respectively.
- The minimization is performed independently for all the pulls of a particular oscillation channel. The total χ^2 for the considered experiment is obtained by repeating the process for all the oscillation channels and their χ^2 values.
- The appearance and disappearance oscillation channels and the respective signal and background events selected for the T2K-II, NOνA-II experiments are given in Tables 3.5 and 3.6, respectively.

- To estimate the total χ^2, we sum up its contribution from all the relevant simulated data samples in an experiment and minimize over the nuisance parameters.

$$\chi^2_{T2K-II(NO\nu A-II)} = Min_{\zeta_s,\zeta_b}\left[\chi^2_{\mu e} + \chi^2_{\mu\mu} + \chi^2_{\bar{\mu}\bar{e}} + \chi^2_{\bar{\mu}\bar{\mu}}\right]$$

For reactor neutrinos from JUNO, we use a Gaussian formula to obatin the value of χ^2 for electron anti-neutrino disappearance channel, given by

$$\chi^2_{\bar{e}\bar{e}} = \sum_{i=1}^{bins}\left(\frac{(N_i^{true} - (1 + a_R + a_D)N_i^{test})^2}{N_i^{true}} + \sum_{j=1}^{R,D}\frac{a_j^2}{\sigma_j^2}\right) \tag{4.5}$$

- a_R and a_D are the small uncertainties in the reactor flux and the fiducial mass of the detector, and their respective standard deviations are σ_R and σ_D. To obtain the χ^2 for JUNO, the $\chi^2_{\bar{e}\bar{e}}$ is summed over four isotopes.

- $\chi^2_{total} = \chi^2_{T2K-II} + \chi^2_{NO\nu A-II} + \chi^2_{JUNO}$ is then minimized over the marginalized oscillation parameters (See Table 4.1) in addition to the systematic parameters (See Table 4.2 and 4.3) to obtain the statistical significance on the hyperplane of parameters of interest.

Table 4.1: Varying $\theta_{13}, \theta_{23}, \delta_{CP}, \Delta m^2_{31}$ for the marginalisation procedure .

Parameter	Range
$\sin^2\theta_{12}$	Fixed
$\sin^2\theta_{13}(\times 10^{-2})$	[0.02034, 0.02430]
$\sin^2\theta_{23}$	[0.4,0.6]
$\delta_{CP}(^\circ)$	$[0, 2\pi]$
$\Delta m^2_{21}(10^{-5}\text{eV}^2/c^4)$	Fixed
$\Delta m^2_{31}(10^{-3}\text{eV}^2/c^4)$	[2.4e-3-2.6e-3 eV^2]

Table 4.2: Systematics of $\nu_\mu(\bar{\nu}_\mu)$ disappearance and $\nu_e(\bar{\nu}_e)$ appearance channels at the FD in T2K-II and NOνA.

Experiments	Signal/BG Normalization error	Calibration Error
T2K-II	3%	0.01%
NOνA-II	5%	2.5%

Table 4.3: Systematics of $\bar{\nu}_e$ disappearance channel in JUNO.

Parameters	Error
Detector norm error	1%
Overall normalization error	1%
Energy scale	1%
Isotopic abundance error	1%

4.3 Mass Hierarchy

The following χ^2 definition are used to study Mass Hierarchy sensitivity studies in this thesis:

$$\chi^2(\delta_{true}) \sim Min(\theta_{23}, \Delta m^2_{31}, \delta_{test}) \sum \left(\chi^2_{\mu e} + \chi^2_{\mu\mu} + \chi^2_{\bar{\mu}e} + \chi^2_{\bar{\mu}\bar{\mu}} + \chi^2_{\bar{e}\bar{e}}\right) \tag{4.6}$$

$$\text{Significance level, } \sigma = \sqrt{\Delta\chi^2} = \sqrt{\chi^2_{NH} - \chi^2_{IH}} \text{ for true hierarchy as normal.} \tag{4.7}$$

- To estimate quantitatively the sensitivity of the experiment(s) to the MH determination, we calculate the statistical significance $\sqrt{\Delta\chi^2}$ to exclude the *inverted* MH given the null hypothesis is a *normal* MH.
- The sensitivity is calculated as a function of *true* δ_{CP} since for the A-LBL experiments, the capability to determine the MH depends on the values of the CP-violating phase.
- Technically, for each *true* value of δ_{CP} with *normal* MH assumed, marginalized χ^2 is calculated for each *test* value of δ_{CP} with the MH fixed *to inverted*.
- Then for each *true* value of δ_{CP} the minimum value of χ^2, which is also equivalent to $\Delta\chi^2$ since the *test* value with *normal* MH assumed would give a minimum χ^2 close to zero, is obtained.

The results, in which we assume $\sin^2\theta_{23} = 0.5$, are shown in Fig. 4-3 for different experimental setups: (i) JUNO only; (ii) NOνA-II only; (iii) a joint of JUNO and NOνA-II; and (iv) a joint of JUNO, NOνA-II, T2K-II and R-SBL experiment. It

is expected that the MH sensitivity of JUNO is more than 3σ C.L. and does not depend on $\delta_{\rm CP}$. On the other hand, the NOνA-II sensitivity to the MH depends strongly on the *true* value of $\delta_{\rm CP}$. A joint analysis of JUNO with the A-LBL experiments, NOνA-II and T2K-II, shows a great boost in the MH determination. This is expected since a joint analysis will break the parameter degeneracy between $\delta_{\rm CP}$ and the sign of Δm^2_{31}. Due to the parameter degeneracy among $\delta_{\rm CP}$, the sign of Δm^2_{31}, θ_{13}, and θ_{23} in the measurement with the A-LBL experiments, we also expect that the MH determination depends on the value of θ_{23}.

The combined sensitivity of all considered experiments at different values of θ_{23}: (i) maximal mixing at 45° ($\sin^2\theta_{23} = 0.50$), (ii) LO at 41° ($\sin^2\theta_{23} = 0.43$), and (iii) HO at 51° ($\sin^2\theta_{23} = 0.60$), is shown in Fig. 4-4. In Fig. 4-5, we compare the MH sensitivity for two hypotheses: MH is *normal* and MH is *inverted*. The result reflects what we expect: (i) the MH resolving with JUNO is less sensitive to its truth since the dominant factor is the separation power between two oscillation frequencies driven by $|\Delta m^2_{31}|$ and $|\Delta m^2_{32}|$ shown in Eq. 4.2 and relatively large mixing angle θ_{12}; and (ii) for the A-LBL experiment like T2K and NOνA, the MH is determined through the MH-$\delta_{\rm CP}$ degeneracy resolving as concisely described in Eq. 4.1. The $A_{\rm CP}$ amplitude is almost unchanged when one switch from *normal* MH to *inverted* MH and simultaneously flip the sign of $\delta_{\rm CP}$. Those results conclude that the *wrong* mass hierarchy can be excluded at greater than 5σ C.L. for all the *true* values of $\delta_{\rm CP}$ and for any value of θ_{23} in the range constrained by experiments. In the other words, the MH can be determined conclusively by a joint analysis of JUNO with the A-LBL experiments, NOνA-II and T2K-II.

As pointed out in Ref. [1], the CPV sensitivity with the A-LBL neutrino experiments does not depend on the the true value of θ_{13}. However this is not the case for the MH sensitivity since the $\overline{\nu}_e$ disappearance rate in JUNO is proportional to $\sin^2 2\theta_{13}$ as shown in Eq. 4.2. This feature is presented in Fig. 4-6 where sensitivity of the neutrino MH are studied with three different values of $\sin^2\theta_{13}$: $\sin^2\theta_{13} = 0.02241$ is the best fit obtained with NuFIT 4.1 [5], $\sin^2\theta_{13} = 0.02221$ is with NuFIT 5.0 [6], and $\sin^2\theta_{13} = 0.02034$ is 3σ C.L. lower limit. Although the neutrino MH sensitivity is slightly reduced with smaller values of $\sin^2\theta_{13}$, the MH

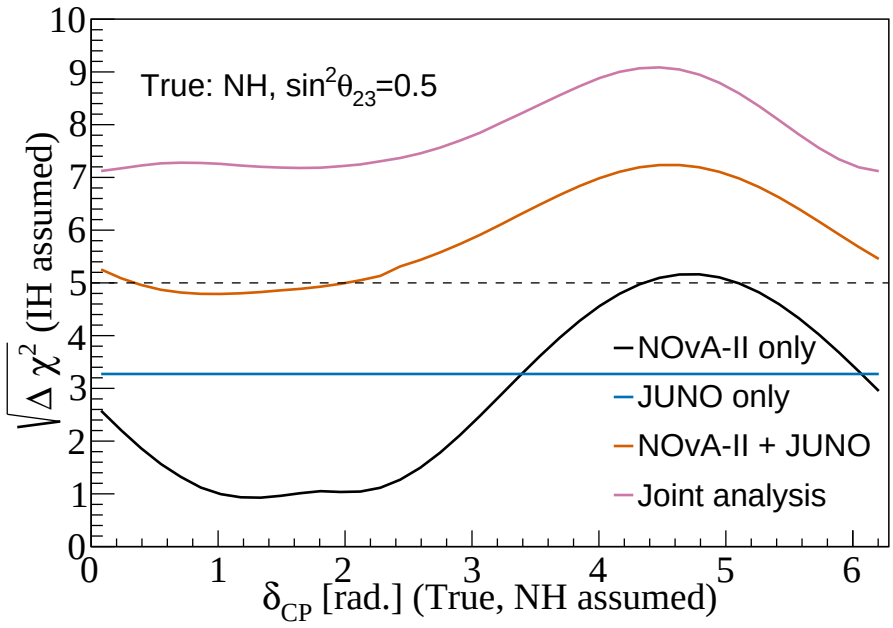

Figure 4-3: MH sensitivities as a function of *true* δ_{CP} calculated for various experimental setups. $\sin^2\theta_{23} = 0.5$ is assumed to be true.

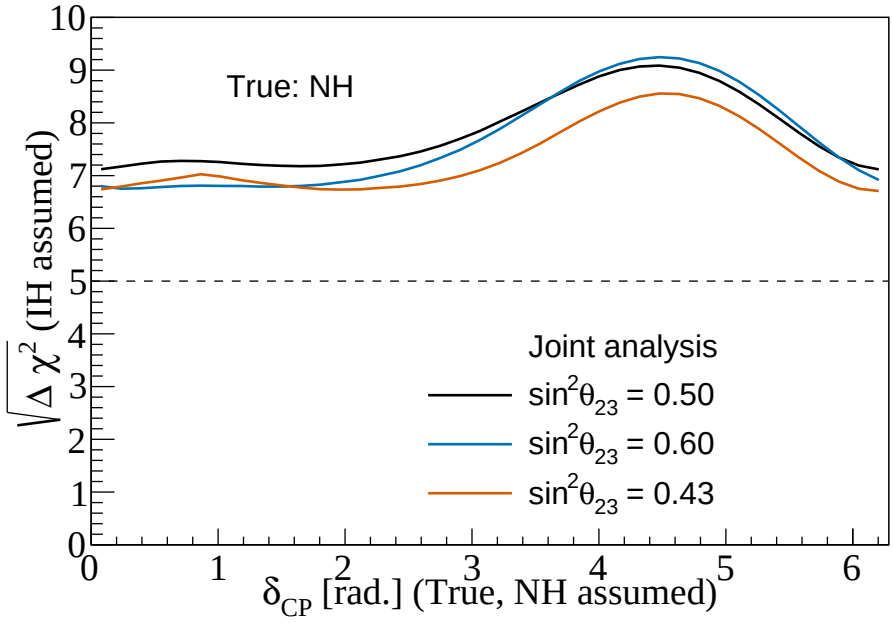

Figure 4-4: MH sensitivities as a function of *true* δ_{CP} calculated for the joint analyses of all considered experiments but at different $\sin^2\theta_{23}$ values.

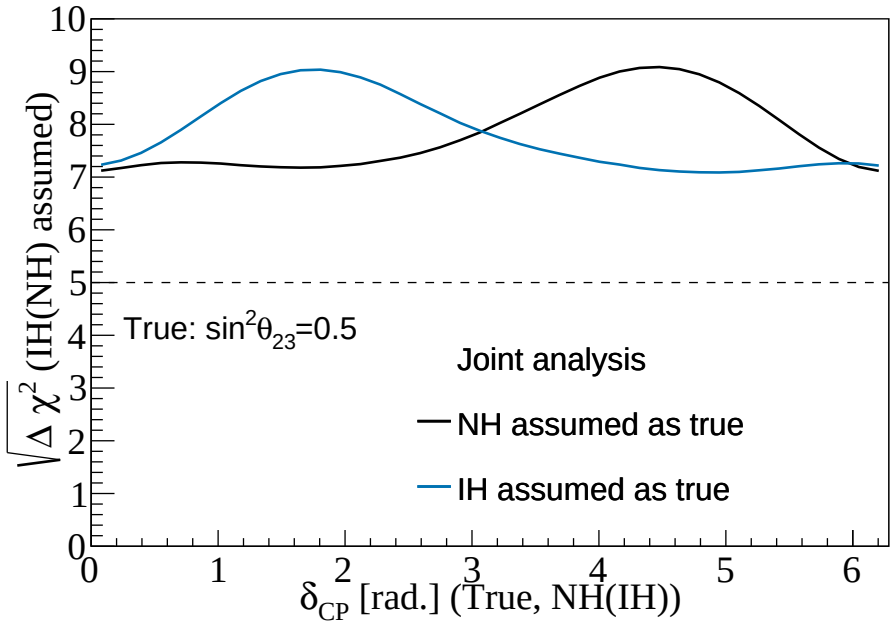

Figure 4-5: MH sensitivities as a function of *true* δ_{CP} calculated for all considered experiments for comparing two possible MH hypotheses. $\sin^2\theta_{23} = 0.5$ is assumed to be true.

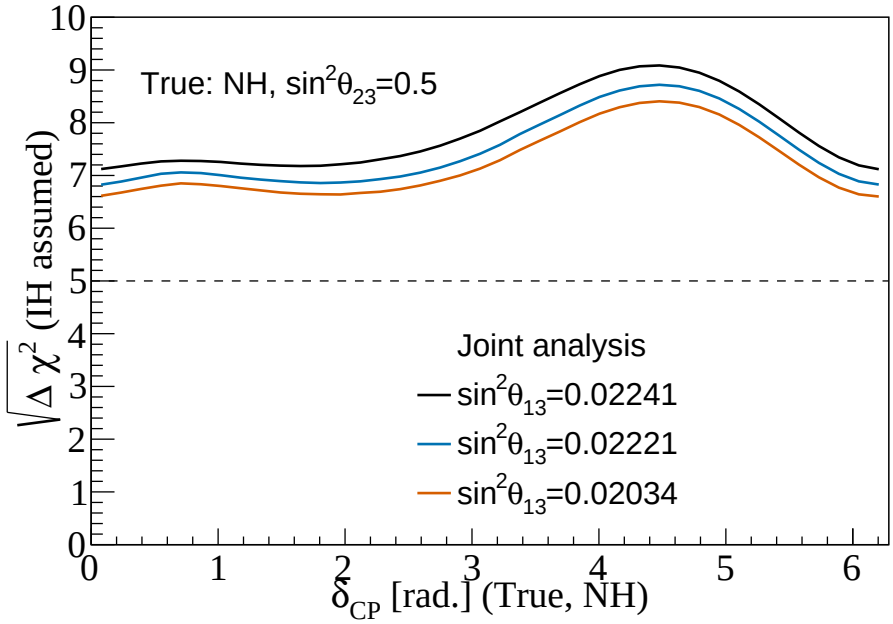

Figure 4-6: Dependence of the neutrino MH sensitivity on the θ_{13} true values: $\sin^2\theta_{13} = 0.02241$ is the best fit obtained with NuFIT 4.1 [5], $\sin^2\theta_{13} = 0.02221$ is with NuFIT 5.0 [6], and $\sin^2\theta_{13} = 0.02034$ is 3σ C.L. lower limit. *Normal* MH and $\sin^2\theta_{23} = 0.5$ are assumed to be true.

resolution is still well above 5σ C.L.

4.4 CP Violation

The statistical significance $\sqrt{\Delta\chi^2}$ to exclude the CP-conserving values ($\delta_{\rm CP}$=0,π) or sensitivity to CPV is evaluated for any *true* value of $\delta_{\rm CP}$ with the *normal* MH assumed.

$$\Delta\chi^2(\delta_{true}) \sim Min\Big(\chi^2_{\rm total}(\delta_{true}) - \chi^2_{\rm total}(\delta_{test} = 0, \pm\pi)\Big) \tag{4.8}$$

For the minimization of χ^2 over the MH options, we consider two cases: (i) MH is *known* and *normal*, same as the truth value or (ii) MH is *unknown*. Fig. 4-7 shows the CPV sensitivity as a function of the *true* value of $\delta_{\rm CP}$ for both MH options obtained by different analyses: (i) T2K-II only; (ii) a joint T2K-II and R-SBL experiments; (iii) a joint of T2K-II, NOνA-II and R-SBL experiments; and (iv) a joint of T2K-II, NOνA-II, JUNO and R-SBL experiments. The result shows that whether the MH is *known* or *unknown* affects on the first three analyses, but not the fourth. This is because, as concluded in the above section, the MH can be determined conclusively with a joint analysis of all considered experiments.

It can be seen that the sensitivity to CP violation is driven by T2K-II and NOνA-II. Contribution of the R-SBL neutrino experiment is significant only at the region where $\delta_{\rm CP}$ is between 0 and π and when the MH is not determined conclusively. JUNO further enhances the CPV sensitivity by lifting up the overall MH sensitivity and consequently breaking the MH-$\delta_{\rm CP}$ degeneracy. At $\delta_{\rm CP}$ close to $-\pi/2$, which is indicated by recent T2K data [7], the sensitivity of the joint analysis with all considered experiments can reach approximately the 5σ C.L.. We also calculate the statistical significance of the CPV sensitivity as a function of *true* $\delta_{\rm CP}$ at different values of θ_{23}, as shown in Fig. 4-8. When *inverted* MH is assumed, although $A_{\rm CP}$ amplitude fluctuates in the same range as when *normal* MH, that the probability and rate of ν_e appearance becomes smaller make the statistic error, $\sigma^{\rm stat.}_{\nu_e}$, lower. In sum, sensitivity to CP violation, which is proportional to $A_{\rm CP}/\sigma^{\rm stat.}_{\nu_e}$, is slightly higher if the *inverted* MH is assumed to be *true* as shown in bottom of the Fig. 4-8.

Table 4.4 shows the fractional region of all possible *true* $\delta_{\rm CP}$ values for which we can exclude CP conserving values of $\delta_{\rm CP}$ to at least the 3σ C.L., obtained by the joint analysis of all considered experiments. Due to the fact

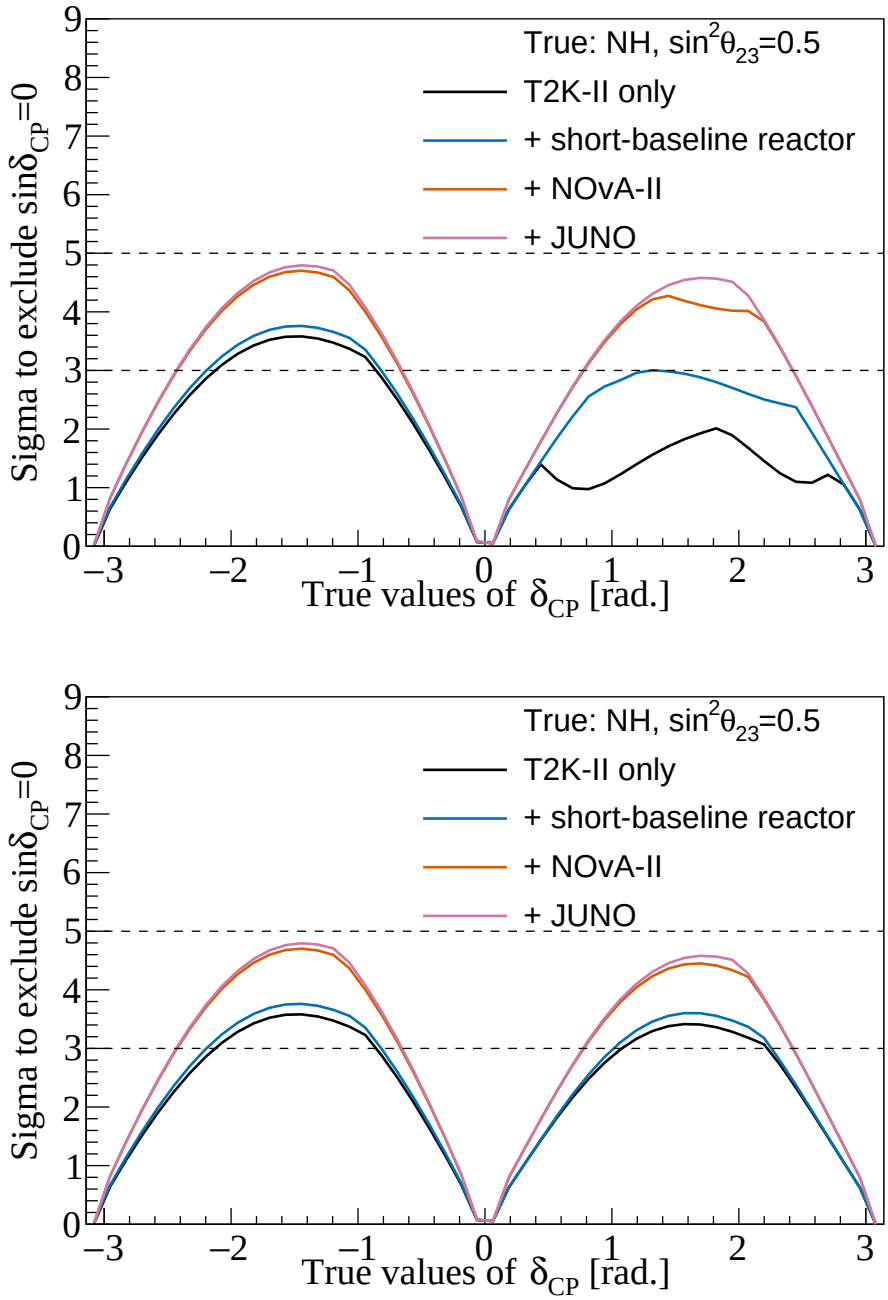

Figure 4-7: CPV sensitivity as a function of the *true* value of δ_{CP} obtained with different analyses. *Normal* MH and $\sin^2\theta_{23} = 0.5$ are assumed to be *true*. Top (bottom) plot is with the MH assumed to be *unknown* (*known*) in the analysis respectively.

that the MH is resolved completely with the joint analysis, the CPV sensitivities are quantitatively identical no matter whether the MH is assumed to be *known* or *unknown*.

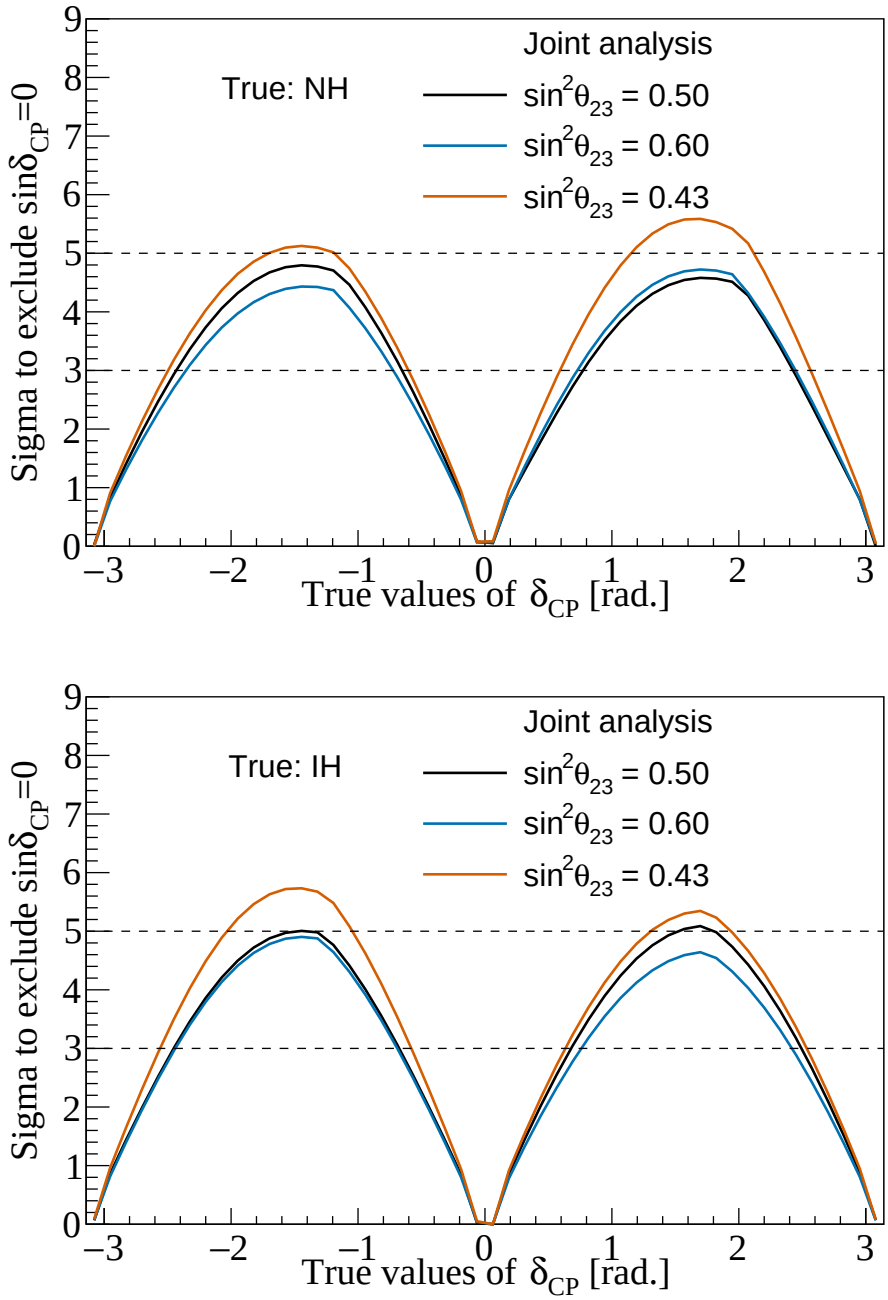

Figure 4-8: CPV sensitivity as a function of the *true* value of δ_{CP} obtained with a joint analysis of all considered experiments at different *true* $\sin^2\theta_{23}$ values (0.43, 0.5, 0.6). Top (bottom) plot is with the *normal* (*inverted*) MH respectively assumed to be true.

Table 4.4: Fractional region of δ_{CP}, depending on $\sin^2\theta_{23}$, can be explored with 3σ or higher significance

Value of $\sin^2\theta_{23}$	0.43	0.50	0.60
Fraction of *true* δ_{CP} values (%), NH	61.6	54.6	53.3
Fraction of *true* δ_{CP} values (%), IH	61.7	57.2	54.2

4.5 Effect of varying exposure of T2K-II on mass hierarchy and CP Violation

Due to the budget issue, it is possible that T2K-II will take data less than the original proposal as discussed in ref. [8]. In this sense, we study three scenarios of the T2K-II POT exposure: 20×10^{21}, 15×10^{21}, and 10×10^{21} POT. While the MH resolving is still well-above 5σ C.L., the CPV sensitivity depends significantly on the POT exposure as shown in Fig. 4-9 and 4-10. However there is still a large fraction of δ_{CP} value excluded with 3σ C.L. The study emphasize the important to provide as many as possible the proton beam to T2K experiment for reaching the highest capability of CPV search.

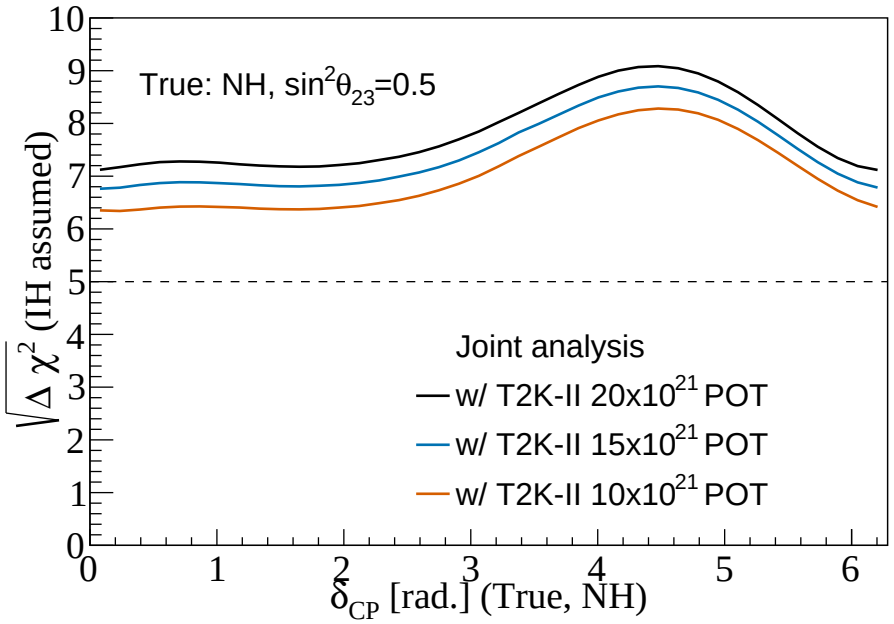

Figure 4-9: Dependence of the combined sensitivity on T2K-II POT exposure on MH sensitivities as a function of *true* δ_{CP} obtained with a joint analysis of all considered experiments. *Normal* MH and $\sin^2\theta_{23} = 0.5$ are assumed to be true.

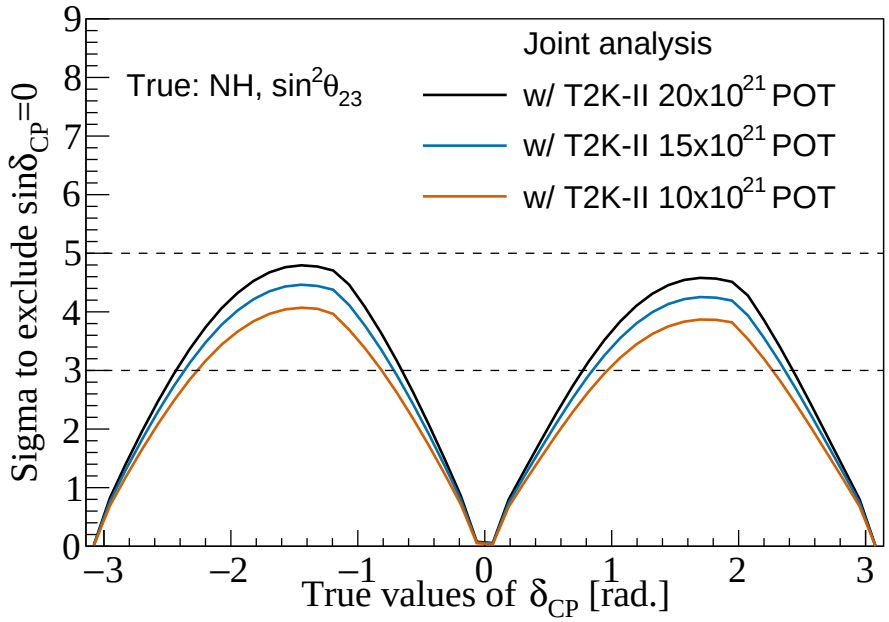

Figure 4-10: Dependence of the combined sensitivity on T2K-II POT exposure on CPV sensitivity as a function of the *true* value of δ_{CP} obtained with a joint analysis of all considered experiments. *Normal* MH and $\sin^2\theta_{23} = 0.5$ are assumed to be true.

4.6 Discussion

We briefly discuss the implications arising from our results in light of the recent updated results from T2K [3], NOvA [2], SK [9], IceCube DeepCore [10], and MINOS(+) [11] presented at Neutrino 2020 conference. T2K prefers the *normal* MH with a Bayes factor of 3.4; SK disfavors the *inverted* MH at 71.4-90.3% C.L.; both NOνA and MINOS(+) disfavor the *inverted* MH at less than 1σ C.L. The prospect of resolving completely the MH by combining T2K-II, NOνA-II and JUNO by 2027 thus is very encouraging. We find out that in Ref. [8] the authors address a similar objective and come to a quite similar conclusion even though a different calculation method and assumption of the experimental setup are used. On the leptonic CPV search, the leading measurement is from T2K where a 35% of δ_{CP}values are excluded at 3σ C.L. Comparing to Ref. [7], although the statistic significance to exclude CP conservation is reduced, from 95% C.L. to 90% C.L., the updated data looks more consistent with the PMNS prediction than before.

While SK also favors the maximum CP violation, NOνA shows no indication of asymmetry of neutrino and antineutrino behaviours. With the combined analysis of T2K-II, NOνA-II, and JUNO by 2027, it is expected that more than half of δ_{CP}values can be excluded with more than 3σ C.L.

Bibliography

[1] Suekane, F. *Neutrino Oscillations: A Practical Guide to Basics and Applications*, vol. 898, 2015.

[2] Himmel, A. New Oscillation Results from the NOνA Experiment, 2020. URL https://doi.org/10.5281/zenodo.4142045.

[3] Dunne, P. Latest Neutrino Oscillation Results from T2K, 2020. URL https://doi.org/10.5281/zenodo.4154355.

[4] Zhan, L. *et al.* Determination of the Neutrino Mass Hierarchy at an Intermediate Baseline. *Phys. Rev. D* **78**, 111103, 2008. 0807.3203.

[5] Esteban, I. *et al.* Global analysis of three-flavour neutrino oscillations: synergies and tensions in the determination of θ_{23}, δ_{CP}, and the mass ordering. *JHEP* **01**, 106, 2019. 1811.05487.

[6] Esteban, I. *et al.* The fate of hints: updated global analysis of three-flavor neutrino oscillations. *JHEP* **09**, 178, 2020. 2007.14792.

[7] **T2K Collaboration** *et al.* Constraint on the matter-antimatter symmetry-violating phase in neutrino oscillations. *Nature* **580** (7803), 339–344, 2020. [Erratum: Nature 583, E16 (2020)], 1910.03887.

[8] Cabrera, A. *et al.* Synergies and prospects for early resolution of the neutrino mass ordering. *Sci. Rep.* **12** (1), 5393, 2022. 2008.11280.

[9] Nakajima, Y. Recent results and future prospects from Super-Kamiokande, 2020. URL https://doi.org/10.5281/zenodo.4134680.

[10] Blot, S. Neutrino oscillation measurements with IceCube, 2020. URL https://doi.org/10.5281/zenodo.4156203.

[11] Carroll, T. Final Long-Baseline Results from MINOS and MINOS+, 2020. URL https://doi.org/10.5281/zenodo.4156118.